NIH Public Access
Author Manuscript
J Comp Neurol. Author manuscript; available in PMC 2010 March 25.

Published in final edited form as:
J Comp Neurol. 2006 June 10; 496(5): 643–654. doi:10.1002/cne.20936.

Dynamic expression of retinoic acid synthesizing and metabolizing enzymes in the developing mouse inner ear

Raymond Romand[1,3], **Takako Kondo**[2], **Valérie Fraulob**[1,3], **Martin Petkovich**[4], **Pascal Dollé**[1,3], and **Eri Hashino**[2]

[1] Institut Clinique de la Souris, B.P. 10142, 67404 Illkirch Cedex, France

[2] Department of Otolaryngology-HNS and Stark Neurosciences Research Institute, Indiana, University School of Medicine, Indianapolis, IN 46202, USA

[3] Institut de Génétique et de Biologie Moléculaire et Cellulaire (CNRS/INSERM/Université Louis Pasteur), B.P. 10142, 67404 Illkirch Cedex, France

[4] Cancer Research Laboratories, Queen's University, Kingston, Ont., Canada K7L 3N6

Abstract

Retinoic acid signaling plays essential roles in morphogenesis and neural development through transcriptional regulation of downstream target genes. It is believed that the balance between the activities of synthesizing and metabolizing enzymes determines the amount of active retinoic acid to which a developing tissue is exposed. In this study, we investigated spatio-temporal expression patterns of four synthesizing enzymes, the retinaldehyde dehydrogenases 1, 2, 3 and 4 (Raldh1, Raldh2, Raldh3 and Raldh4) and two metabolizing enzymes (Cyp26A1 and Cyp26B1) in the embryonic and postnatal mouse inner ear using quantitative RT-PCR, *in situ* hybridization and Western blot analysis. Quantitative RT-PCR analysis and Western blot data revealed that the expression of CYP26s was much higher than that of Raldhs at early embryonic ages, but that Cyp26 expression was down-regulated during embryonic development. Conversely, the expression levels of Raldh2 and -3 increased during development and were significantly higher than the Cyp26 levels at postnatal day 20. At this age, Raldh3 was expressed predominantly in the cochlea, while Raldh2 was present in the vestibular end organ. At early embryonic stages as observed by *in situ* hybridization, the synthesizing enzymes were expressed only in the dorsoventral epithelium of the otocyst, while the metabolizing enzymes were present mainly in mesenchymal cells surrounding the otic epithelium. At later stages, Raldh2, Raldh3 and Cyp26B1 were confined to the stria vascularis, spiral ganglion and supporting cells in the cochlear and vestibular epithelia, respectively. The downregulation of Cyp26s and the upregulation of Raldhs after birth during inner ear maturation suggests tissue changes in the sensitivity to retinoic acid concentrations.

Keywords

Raldh1; Raldh2; Raldh3; Raldh4; Cyp26A1; Cyp26B1; *in situ* hybridization; RT-PCR; Western blot; cochlea; vestibular organ?

To whom correspondance should be sent: R. Romand, Institut Clinique de la Souris and Institut de Génétique et de Biologie Moléculaire et Cellulaire, B.P. 10142, 67404 ILLKIRCH CEDEX, France. Tel.: (33) 388 65 56 67 Fax : (33) 388 65 32 01 E-mail : romand@igbmc.u-strasbg.fr.

NIH-PA Author Manuscript
NIH-PA Author Manuscript
NIH-PA Author Manuscript

NIH-PA Author Manuscript
NIH-PA Author Manuscript
NIH-PA Author Manuscript

Introduction

Vitamin A (retinol) and its active metabolite retinoic acid (RA) are essential for normal development of vertebrate embryos (Means and Gudas, 1995; Ross et al., 2000). RA (in its all-*trans* and/or 9-*cis* forms) is the ligand for two families of nuclear receptors, the RARs (α, β, and γ) and RXRs, (α, β, and γ). RARs and RXRs act in heterodimeric combinations to transduce the retinoid signal and regulate the transcription of target genes via DNA regulatory sequences (Chambon, 1996; Perlmann and Evans, 1997). Although retinoid signaling requires these receptors (see Ross et al., 2000), the effectiveness of this signaling is regulated by the balance between RA synthesis and metabolism during embryogenesis (McCaffery et al., 1999; Blentic et al., 2003). Normal embryonic development requires appropriate tissue distributions of RA, and both excess and deficiency result in developmental anomalies (Maden, 1994; 2002; and refs. therein). Thus, RA supply must be precisely controlled through stage- and tissue-specific expression of both synthesizing and metabolizing enzymes.

Physiologically inactive retinol is converted into RA by two oxidative reactions. Retinol is oxidized into retinaldehyde by members of the alcohol dehydrogenase (Adh) family, after which retinaldehyde is converted into RA by four enzymes known as retinaldehyde dehydrogenases (Raldh) 1, 2, 3 and 4 (Duester, 2000; Lin et al., 2003). The biosynthesis step seems to be a limiting factor for RA availability in a given tissue. For example, there is a close relationship between embryonic expression patterns of *Raldh* genes and those of a RA-reporter transgene (Niederreither et al., 2002a; Mic et al., 2003). In addition, mutant mouse embryos deficient for Raldh2 show developmental abnormalities similar to those observed in embryos deprived of retinoids (Niederreither et al., 1999; White et al., 2000). RA is metabolized into more polar (4-hydroxy and 4-oxo) derivatives by three members of the cytochrome P450 superfamily, Cyp26A1, -B1 and -C1 (Fujii et al., 1997; White et al., 1997; 2000; Sakai et al., 2001). Targeted disruption of *Cyp26A1* in the mouse leads to a lethal malformative phenotype that recapitulates some of the teratogenic effects of RA, consistent with the idea that this enzyme is required to trigger the tissue-specific catabolism of endogenous RA (Abu-Abed et al., 2001; Sakai et al., 2001). Interestingly, the *Cyp26A1*$^{-/-}$ phenotype can be partially rescued by heterozygous disruption of the *Raldh2* gene, which decreases the amounts of RA synthesized within the embryo (Niederreither et al., 2002b), further indicating that the primary function of *Cyp26s* is to protect tissues from excess exposure to RA (Niederreither et al., 2002b). Moreover, the local balance between Raldh and Cyp26 activities may be responsible for the asymmetric distribution of RA in some developing structures, such as the embryonic retina (McCaffery et al. 1999). These observations indicate that both the synthesis and metabolism of RA need to be precisely controlled to accomplish normal developmental programs (Stoilov, 2001; Perlmann, 2002).

In a previous study, we have shown complementary expression patterns of *Raldh* and *Cyp26* genes in the mouse inner ear at embryonic day 18.5 (Romand et al., 2004). This study did not address expression of *Raldhs* and *Cyp26s* at earlier developmental stages, when cell fate determination and inner ear patterning are underway. Characterizing the expression patterns of genes encoding the enzymes involved in RA homeostasis may give insights into the functions of RA in the developing inner ear. In the present work, we have studied the expression profiles of *Raldh* and *Cyp26* genes throughout development of the mouse inner ear using *in situ* hybridization (ISH) and immunohistochemistry. In addition, we have analyzed temporal changes in the expression level of these metabolic enzymes using non-quantitative and quantitative RT-PCR and Western blots analysis. Our study has revealed dynamic and often complementary expression patterns for each member of the Raldh and Cyp26 families, suggesting that the expression of each enzyme is controlled independently.

NIH-PA Author Manuscript

NIH-PA Author Manuscript

NIH-PA Author Manuscript

Materials and Methods

Mouse tissue collection and sample preparation

The spatio-temporal distribution of *Raldh* and *Cyp26* transcripts was analyzed by *in situ* hybridization of cryosections from CD1 mouse embryos and fetuses at embryonic day (E) 9.5, 10.5, 12.5, 14.5 and 18.5. Pregnant females (morning of vaginal plug was considered as E0.5) were sacrificed by cervical dislocation and fetuses were collected in phosphate-buffered saline (PBS) after cesarian section. The specimens were stored in methanol (for whole-mounts) or placed in molds containing Tissue-tek embedding medium (Sakura Finetek, Torrance, CA) and frozen on the surface of dry ice, as previously described (Niederreither and Dollé, 1998). Serial sagittal 10 μm sections were collected on Superfrost slides and stored at -80°C until use. Animal care and experimentation were carried out according to the guidelines of the European Union.

In situ hybridization

The detailed procedures for ISH with radioactive probes have been described (Niederreither and Dollé, 1998). The antisense (or sense) RNA probes were transcribed by standard T7, T3 or SP6 polymerase reactions, using [α^{35}S]-CTP (Amersham, Buckinghamshire, England), followed by partial alkaline hydrolysis to reduce the average probe length to ca. 150 nucleotides. The DNA templates used in these reactions have been described previously (Niederreither et al., 1997; 2002c; MacLean et al., 2001). Adjacent serial sections were hybridized to various probes in order to analyze the entire inner ear. Sense probes were also tested in order to determine background levels. The sections were examined using a Leitz microscope, under brightfield illumination for histology, and darkfield illumination to vizualize autoradiography silver grains. Expression domains are displayed as computer superimpositions of brightfield views showing histology (toluidine blue staining) and darkfield views revealing the signal grains (displayed in false red-brown color) using Adobe Photoshop software. ISH was performed on E9.5 embryo sections using digoxigeninlabelled probes, and the robotic procedure described in Carson et al. (2002).

RT-PCR

Inner ear tissues were collected from CD1 mice at E9, E10, E12, E14, E18 and postnatal day 5 (P5) and P20, and stored in RNA later (Ambion). For E18, P5, P20 tissues, the cochlear and vestibular portions of the inner ear were dissected and stored separately. Total RNA was isolated from tissues using the RNeasy Mini-kit (QIAGEN) according to the manufacturer's protocol. Following extraction, all samples were treated with TURBO DNase (Ambion) to avoid DNA contamination. Single-stranded cDNA was synthesized using Omniscript reverse transcriptase (Qiagen) and oligo-dT primers at 37°C for 60 min. For non-quantitative RT-PCR, cDNA samples were amplified using the Thermoscript RT-PCR system (Invitrogen). For quantitative RT-PCR, experiments were run on an ABI PRISM 7900HT Sequence Detection System (Applied Biosystems) using SYBR Green as a reporter. The cDNA samples were mixed with the SYBR Green PCR Master Mix (Applied Biosystems) that contains dNTPs with dUTP, AmpliTaq Gold DNA polymerase, AmpErase UNG, optimized buffer and SYBR Green. For each PCR reaction, a mixture containing cDNA template (5 ng), Master Mix (1×) and forward and reverse primers (400 nM) was placed in a 96 well MicroAmp Optical Reaction Plate with all experimental samples in quadruplicate and all standard curves in triplicate. The primers used in this study were: *Raldh1* (forward 5′-TTTATCATCAAGGCCAATGC-3′ and reverse 5′-CTTAGCTCGCTCAACACTCCT-3′), *Raldh2* (forward 5′-GACTTGGACTACGCTGTGGA-3′ and reverse 5′-TCTTCCACAAAGATGCGAGA-3′), *Raldh3* (forward 5′-CGAAGAGTGCGAACCAGTTA-3′ and reverse 5′-CTTGGTGAACTTGACCTCCA-3′), *Raldh4* (forward 5′-

NIH-PA Author Manuscript

NIH-PA Author Manuscript

NIH-PA Author Manuscript

ATCAGCCCTTGGAATTTACC-3′ and reverse 5′-AAGTCATCTCACTGGGCTTG-3′), *Cyp26A1* (forward 5′-AGCAGCGAAAGAAGGTGATT-3′ and reverse 5′-TAGCCACTGCTCCAGACAAC-3′) and *Cyp26B1* (forward 5′-CGCTACCTGGACTGTGTCAT-3′ and reverse 5′-GGATCTGGAAACCATCCAGT-3′). In most cases, the PCR reaction was run under the following conditions: 1×, 50°C, 2 minutes; 1×, 95°C, 10 minutes; 55×, 95°C, 15 seconds, 60°C, 1 minute; 1×, 72°C, hold. After amplification, the PCR products were analyzed with ABI PRISM sequence detection software. To check the linearity of the detection system, a cDNA dilution series (1, 1/10, 1/100, 1/1000) was amplified with a primer pair and a correlation coefficient was calculated from the standard curve that displays threshold cycles (C_T) as a function of $\log_{10}$ cDNA concentrations. The mRNA level for each probe (x) relative to L27 mRNA (a housekeeping gene used as internal control) was calculated as follows: $\text{mRNA}(x) = 2^{\text{Ct (L27)-Ct(x)}} \times 100$.

Western blot

Proteins were extracted from E10, E18, and P20 mouse tissues by homogenization in RIPA buffer (50 mM Tris-HCl, pH 8.0, 150 mM NaCl, 0.5% deoxycholic acid, 1% SDS, 1% NP40) with 1× Halt™ Protease Inhibitor Cocktail (Pierce, Rockford, IL). The protein concentration of the lysates was determined by the BCA technique (Pierce). Total protein (10 μg/lane) was loaded on a 10% polyacrylamide gel, separated by SDS-PAGE, and then blotted onto Immun-Blot PVDF membranes (Bio-Rad, Hercules, CA). Western blotting was performed by blocking the membrane in Blocking Buffer (5% non-fat milk in TBST), then incubating in primary antibody diluted Blocking Buffer. Antibodies and dilutions used were: anti-CYP26A1 (1:2000), anti-Raldh2 (1:1000), anti-Raldh3 (1:1000). The anti-Raldh2 and anti-Raldh3 antibodies (a kind gift of Drs. U. Dräger and P. McCaffery) have been previously characterized and have been used in various expression studies(e.g. Berkovitz et al., 2001; Wagner et al., 2002; Luo et al., 2004). The CYP26A1 antibody (M.P., unpublished) was targeted against the epitope VDNLPARFTYFQGDI, and was tested (i) in Western blot assays performed on lysates from bacteria overexpressing either mouse or human CYP26A1s; and (ii) by immunocytochemistry of COS cells transfected either with a Cyp26A1 or a Cyp26B1 expression vector. Only the Cyp26A1-transfected cells gave a detectable immunofluorescence signal (M.P., unpublished data). An anti-β-actin antibody (1:5000, Sigma, St. Louis, MO) was also used to ensure equal loading of lanes. The membranes were then washed and incubated in anti-rabbit IgG-HRP. The signal was developed using the SuperSignal® West Femto substrate (Pierce).

Immunohistochemistry

Embryos were slightly prefixed in 4% PFA and cryoprotected in sucrose. 10 μm cryostat sections were treated with anti-Raldh2 and 3 antibodies, followed with goat anti-rabbit IgG conjugated with Alexa 488 (Molecular Probes, Eugene OR). Diamidino-phenyl-indole (DAPI) nuclear labelling was achieved in some cases by incubating the sections in the dye solution for 2 minutes. Nonimmune control sections were similarly treated with omission of primary antibodies. Fluorescent labelling was observed by using a Leica Spectra SP1 confocal microscope with excitation/emission wavelengths set at 488/518 nm for fluoresceine and 351/461 for Alexa TM 488. Image processing was achieved with Photoshop 7.0.

Results

RT-PCR analysis

Using non-quantitative RT-PCR, we assessed whether *Raldh1-4*, *Cyp26A1* or *Cyp26B1* mRNA is expressed in the developing inner ear and, if so, how the expression level of each mRNA in the inner ear evolves during embryonic and postnatal development (Fig. 1).

NIH-PA Author Manuscript

NIH-PA Author Manuscript

NIH-PA Author Manuscript

Expression of *Raldh1*, *Raldh2*, *Raldh3*, *Cyp26A1* and *Cyp26B1* mRNAs was detected at least at some stage of inner ear development, whereas *Raldh4* mRNA was not detectable at any stage examined (Fig. 1). Both *Raldh2* and *Raldh3* were detectable at all developmental stages from E9 to P20, while *Raldh1* level was very low and barely detectable at E18 only. Expression levels of *Cyp26A1* and *Cyp26B1* were high at early embryonic stages, but declined and became undetectable after E14 and P5, respectively. Comparison of *Raldh1* level between the otocyst and the optic placode at E10 where this enzyme was known to be well expressed (Li et al., 2000), showed a strong expression in the optic placode while no expression was present in the otocyst (data not shown).

Quantitative RT-PCR analysis was performed to evaluate the mRNA level of each Raldh and Cyp26 enzyme in the E10, E18 and P20 cDNA samples (Fig. 2). At E10, *Cyp26A1* mRNA level was the highest (2.0% of the *L27* control mRNA), followed by *Cyp26B1* (0.4% of *L27* mRNA). Compared to *Cyp26s* expression in the E10 otocyst, *Raldhs* mRNA levels were generally low: *Raldh3* and *Raldh2* mRNA levels were 0.1% and 0.07% of the *L27* mRNA level, respectively. At E18, expression levels of *Cyp26A1*, *Raldh1* and *Raldh4* were very low or undetectable. In contrast, *Cyp26B1*, *Raldh2* and *Raldh3* were detected in both vestibular and cochlear partitions in the inner ear. No significant difference in tissue level was detected for *Cyp26B1* between the vestibular vs. the cochlear partition, whereas the *Raldh2* and *Raldh3* levels in the vestibular partition were clearly higher than those in the cochlear partition. At P20, the *Cyp26A1* level was extremely low both in the cochlea and vestibule, while *Cyp26B1* in the vestibule remained at a moderate level (0.3% of *L27*). Contrasting with the down-regulation of *Cyp26A1* and *-B1*, the levels of *Raldh2* and *Raldh3* at P20 were significantly higher than at E10. Interestingly, *Raldh3* had a four-fold higher level in the cochlea compared to the vestibule, while *Raldh2* had a 3-fold higher level in the vestibule (Fig. 2).

Western blot analysis

Using Western blot analysis, we examined whether the temporal expression patterns of *Raldh2*, *Raldh3*, and *Cyp26A1* transcripts correlate with their respective protein levels. Comparison across stages revealed that both Raldh2 and Raldh3 were sharply up-regulated from E10 to E18, after which they were slightly down-regulated by P20 (Fig. 3). At E18 and after birth, Raldh3 was present at a lower level in the cochlear region compared to the vestibular partition. In contrast, Cyp26A1 was clearly detected at E10, but then was down-regulated by E18 and was barely detectable at P20.

In situ hybridization analysis

At E9.5, *Raldh1* expression was restricted toward the dorsal region of the otocyst extending toward the caudal region (Fig. 4A). Highest expression was seen in the optic vesicle and foregut epithelium (data not shown). At E10.5, *Raldh1* signal was present in the endolymphatic duct primordium, which was visible as an outgrowth of the dorsal otocyst epithelium (Fig. 5A). Transcripts were also observed in the ventro-lateral region of the otocyst (data not shown; see Fig. 6A). At E12.5, *Raldh1* signals were localized primarily in the endolymphatic duct and the lateral otic epithelium (Figs. 5F, 6B). Later on, when the vestibular components of the inner ear were differentiated from the cochlear ones (E14.5 and E18.5), *Raldh1* transcripts were present in all the epithelia lining the semicircular canals (Figs.5K, 6C-D), the crus commune and the endolymphatic duct, but not in the endolymphatic sac (data not shown). Transcripts were also detected in the lateral border of cristae at E14.5 (Fig. 5K). At E18.5, *Raldh1* was still observed in the same region of the cristae, plus the lateral regions of the utricular and saccular maculae which may correspond to the transitional epithelia (Fig. 6D). Transcripts were excluded from the differentiating sensory epithelia (data not shown, see Romand et al., 2004).

NIH-PA Author Manuscript

NIH-PA Author Manuscript

NIH-PA Author Manuscript

Raldh2

Raldh2 transcripts were weakly expressed in the dorsal otocyst at E9.5 (Fig. 4B), although strong signals were present in somites and lateral plate mesoderm, as previously described (Niederreither et al., 1997). At E10.5, *Raldh2* transcripts were detected on cross-sections in a small domain of the lateral otic epithelium (Figs. 5B, 6A), after which the expression expanded dorso-ventrally along the lateral side of the otic epithelium (data not shown; see Fig. 6B). The *Raldh2*-positive domain was localized in the otic epithelium that gives rise primarily to the cochlea. At E14.5, ISH signals were observed in epithelial regions adjacent to the crista ampullaris (Fig. 5L). Positive signals were also observed in non-sensory regions of the cochlea (Fig. 6C). At E18.5, *Raldh2* expression was confined to the stria vascularis and the Reissner membrane in the cochlea (Figs. 4F, 6D), while the expression domain in the vestibular region was similar to that observed at E14.5. ISH signal was also present in the utricule (data not shown; see Fig. 6D).

Raldh3

In the E9.5 embryo, *Raldh3* was expressed in the dorsal part of the otocyst extending toward the rostral and ventral regions (Fig. 4C). The ISH signal was low in comparison to that observed in the optic vesicle and nasal region (data not shown). At E10.5, *Raldh3* transcripts were restricted to two domains in the otocyst, one in the dorso-medial region corresponding to the vestibular sensory region adjacent to the endolymphatic duct primordium, and another in the ventral region of the otic epithelium (Figs. 5C; 6A). Later at E12.5, positive labeling was observed in three separate regions in the otic epithelium: (1) the medial otic epithelium corresponding to the endolymphatic duct and adjacent prospective vestibular sensory epithelium, (2) the lateral region just beneath the beginning of the horizontal semicircular canal and (3) the ventral region corresponding to the presumptive cochlear sensory epithelium and ganglion (Figs. 5H, 6B). At E14.5 and E18.5, the lower part of the endolymphatic duct exhibited strong *Raldh3* labeling (data not shown). *Raldh3* transcripts were also present in the baso-lateral region of the crista (Figs. 5M, 6C, D). In most samples, signals were also detected in the lateral regions of the saccular and utricular sensory epithelia (Figs. 5M, 6C, D). In the cochlea, *Raldh3* was strongly expressed in the spiral ganglion (Figs. 6C, D). A lower ISH signal was observed in the cochlear nerve and the stria vascularis (data not shown). No signal was detected in the cochlear sensory epithelium.

Raldh4

No *Raldh4* expression was observed in the otocyst and inner ear at any developmental stage examined, although we observed *Raldh4* expression in the liver at E14.5 and E18.5 (data not shown; see Lin et al., 2003).

Cyp26A1

Strong *Cyp26A1* expression was observed in the tail bud and branchial arches of the embryo as early as E9.5 (data not shown). Expression was also found in the axial mesenchyme caudal and ventral to the otocyst and in a restricted caudal region of the otic epithelium (Fig. 4D). At E10.5, strong *Cyp26A1* signals were seen in mesenchymal tissues surrounding the lateral and ventral domains of the otocyst, as well as in the ventral otic epithelium that gives rise to the cochlear epithelium (Figs. 5D, 6A). Two days later, *Cyp26A1* expression remained strong in the mesenchyme surrounding all semi-circular canals and the ventral region of the otocyst (Figs. 5I, 6B). At E14.5, *Cyp26A1* transcripts were confined to the endolymphatic duct, the tissues surrounding the round window membrane and beneath the sensory epithelium in the sacculus (Fig. 6C). In the cochlear region, *Cyp26A1* was present only in the cochlear epithelium (Fig. 6C). However, at E18.5, no transcripts were detected in the inner ear, except in the endolymphatic duct (Fig. 6D and data not shown).

NIH-PA Author Manuscript

NIH-PA Author Manuscript

NIH-PA Author Manuscript

Cyp26B1

At E9.5, *Cyp26B1* expression was observed in the forelimb bud, the branchial arches and was highest in hindbrain cells of rhombomeres 5 and 6, that are adjacent to the otocyst (Fig. 4E; MacLean et al., 2001). Transcripts were weakly expressed in the dorsal half of the otic epithelium (Fig. 4E). At E10.5, *Cyp26B1* expression domains in the otocyst epithelium were much more restricted when compared to *Cyp26A1*. *Cyp26B1* transcripts were present in two focal regions corresponding to the prospective cochlear sensory epithelium and the lateral part of the otic epithelium opposite to the prospective vestibular sensory epithelium (Figs. 5E, 6A). At E12.5, *Cyp26B1* was expressed in a small region of the vestibular sensory epithelium and in the mesenchyme surrounding the horizontal semi-circular canal (Figs. 5J, 6B). At stages ranging from E14.5 to E18.5, *Cyp26B1* signals were confined to the sensory epithelia in the saccule, the utricule, the cristae and the cochlea (Figs. 5O, 6C, D).

Immunohistochemistry

As transcript distributions may not always give an accurate picture of protein expression in a specific tissue, Raldh2 and Raldh3 proteins were examined at E18.5 by immunohistochamistry, in order to confirm if their presence and their localization match those of their transcripts. Consistent with our ISH data showing that *Raldh2* transcripts are confined the stria vascularis at this stage of development (Fig. 6; Romand et al., 2004), immunohistochemistry confirmed the presence of Raldh2 in the same tissue (Fig. 4F), indicating that RA may be specifically synthesized in this part of the cochlea. Likewise, Raldh3 whose transcripts are confined to the spiral ganglion (Fig. 6;Wagner et al., 2002;Romand et al., 2004) was present in the cell bodies of spiral ganglion neurons (Fig. H). No Raldh3 immunoreactivity was observed in satellite cells and fibers from the efferent bundle (Figs. 4G, H).

Discussion

Retinoic acid is a master signalling molecule that controls embryonic development through transcriptional regulation of an array of downstream target genes, such as growth factors and extracellular matrix proteins (Gudas, 1994; McCaffery and Dräger, 2000). Previous studies have shown that local concentrations of RA at a given embryonic stage are controlled by the balance between the activities of RA synthesizing and metabolizing enzymes, while the tissue sensitivity to RA is determined by the expression levels of its nuclear receptors. The Raldhs and Cyp26s enzymes are responsible for RA synthesis and catabolism, respectively, and play major roles in RA homeostasis (McCaffery and Dräger, 2000, and refs. therein). It is believed that the tissue distribution of these enzymes is precisely controlled to yield optimal RA levels in RA-responsive cells. Based on this assumption, a reduction or loss of Raldhs or Cyp26s activity would result in developmental anomalies, but these abnormal phenotypes could be rescued by increasing or decreasing RA concentrations, respectively. In favour of this hypothesis, developmental anomalies seen in *Raldh2* knockout mice, including defects in hindbrain, somites, heart and forelimb buds, can be partially rescued by feeding the pregnant mothers with subteratogenic doses of RA (Niederreither et al., 1999 and 2000). Conversely, the tail bud truncation and skeletal malformations characteristic of *Cyp26A1* knockout mice (Abu-Abed et al., 2001; Sakai et al., 2001) were rescued by crossing this line with *Raldh2* heterozygous mutants (Niederreither et al., 2002b). These rescue experiments validated a critical role for Raldhs and Cyp26s in generating appropriate distributions and levels of RA available to each cell or tissue at a given embryonic stage, thereby ensuring normal developmental processes.

To provide insights into a role for RA signaling in morphogenesis and cell fate determination in the developing inner ear, we have performed a comprehensive analysis of

NIH-PA Author Manuscript

NIH-PA Author Manuscript

NIH-PA Author Manuscript

the expression of *Raldhs* and *Cyp26s* at various developmental stages. Our *in situ* hybridization analysis revealed that *Raldhs* and *Cyp26A1* are very often confined to different tissues in the early stage otocyst: between E9.5 and E12.5 *Raldh-1*, *-2* and *-3* are expressed only in the otic epithelium, while *Cyp26A1* is mainly confined to mesenchymal tissues surrounding the otic epithelium (Figs. 4A-D, 5A-J, 6A-B). However, some areas of co-localization are also observed, for instance between *Raldh1* and *Cyp26A1* in the ventral region of the otic epithelium (Figs. 5A and I), and between the two Cyp26s in mesenchymal tissues around the horizontal semi-circular canal and the cochlea (Figs. 5I-J, 6B). When the *Raldh* expressions are compared with that of *Cyp26s*, it looks as if the synthesizing enzymes epithelial expression domains in the ventro-lateral region of the developing inner ear delineate a narrow margin surrounded by a wide mesenchymal region expressing metabolizing enzymes (see Figs. 6A-B). This suggests that RA levels must be tightly controlled in the presumptive cochlear epithelium. One possibility is that the *Cyp26*-positive regions metabolize RA that could otherwise diffuse out toward the mesenchyme, thereby preventing RA to reach this tissue. However, there are observations that RA is important for periotic mesenchyme condensation (Frenz et al., 1997; Butts et al., 2005). Another more likely possibility is that metabolizing enzymes could restrict RA signaling in cells residing in the inner ear epithelium. It is possible that the function of Cyp26s is to prevent RA influx from outside the otocyst so that the otocyst could function as a closed system with no need for external RA during early development. Along this line of evidence, Choo et al., (1998) showed that RA treatement of wild-type embryos resulted in embryopathy of the otocyst, presumably due to transient modification of its endogenous distribution in some parts of the embryonic inner ear. In addition, a recent study utilizing a RA-responsive *lacZ* reporter transgene revealed that Cyp26s can act as local inhibitors of RA signaling. In this study, *lacZ* activity was shown to be absent in a stripe of the embryonic retina where Cyp26s are expressed during development (Sakai et al., 2004). However, when embryos are exposed to exogenous RA, the *lacZ*-negative stripe becomes transiently obliterated and intense *lacZ* expression is also observed in adjacent regions (Luo et al., 2004). It was concluded that excess RA overrides the metabolizing capacity of Cyp26 enzymes, resulting in ectopic activation of RA signaling in the retina. A similar function of Cyp26 enzymes may be required to confine RA signaling in the presumptive cochlear epithelium, where it could act for cell fate specification or cochlear sensory differentiation. A third possibility which cannot be formally ruled out is that Cyp26 activity may lead to the production, in a region-specific manner, of novel active RA metabolites such as 4-oxo RA (Pijnappel et al., 1993; Achkar et al., 1996). So far, however, there has been no genetic evidence for a role of such ‘alternative’ RA compounds in the mouse (Sakai et al., 2001; Abu-Abed et al., 2001; Niederreither et al., 2002b).

During development, reciprocal interactions between the periotic mesenchyme and the otic epithelium are thought to play an important role in pattern formation of the inner ear (Noden and Van de Water, 1992; Frenz and Liu, 1997). Examples of signaling molecules known to be involved in the mesenchyme-epithelium interactions at early stage of ear development include TGFβ_1 (Frenz et al., 1992; Paradies et al., 1998), FGFs (Frenz et al., 1994, Wright and Mansour, 2003), BMPs (Frenz et al., 1996b; Morsli et al., 1998; Chang et al., 2002; Liu et al., 2003) and Shh (Riccomagno et al., 2002; Liu et al., 2002). It is interesting to note that RA regulates the expression of growth factors and growth factor receptors (Gudas 1994; Yoshizawa et al., 1998; Sizemore et al., 1998; McCaffery et al., 2000), as well as the transcription rate of the *Shh* and *Bmp4* genes via RAREs in their promoters (Chang et al., 1997; Thompson et al, 2003). Thus, limiting the availability of RA to the otic epithelium could conceivably generate differences in the concentrations of some of the signaling proteins downstream of RA. According to this hypothesis, it is possible that an alteration in RA levels during early embryogenesis would compromise epithelium-specific expression of these downstream targets, thereby disrupting the normal morphogenetic program (Jarvis et

NIH-PA Author Manuscript

NIH-PA Author Manuscript

NIH-PA Author Manuscript

al., 1990; Burk and Willhite, 1992; Frenz et al., 1996a; Choo et al., 1998; Pasqualetti et al., 2001). Such RA-mediated interactions between mesenchyme and epithelia appear to be essential for the development of other structures, since heart, limb, face and forebrain development are also disrupted by anomalous RA exposure (Lannoue et al., 1997; te Welscher et al., 2002; Dudas et al., 2004). Furthermore, instances of human birth defects with inner ear embryopathy are often associated with malformations of the limbs, heart and face (La Mantia, 1999; Underhill et al., 2001; Vermot et al., 2003; Yashiro et al., 2004).

Our quantitative RT-PCR analysis is consistent with the ISH patterns observed for the most of the enzymes investigated. For example no or very low levels of *Raldh4* mRNA transcripts were observed at any stage by both techniques. However, in the case of *Raldh1* there is a poor consistency between PCR and ISH patterns, that could be explained by different thresholds of sensitivity. The comparative importance of different Raldhs during development can be seen from gene inactivation studies. Knockout of the *Raldh2* gene results in early embryonic lethality (Niederreither et al., 1999), while *Raldh3* knockout mice die at birth (Dupé et al., 2003), and *Raldh1* deletion does not lead to a detectable abnormal phenotype (Fan et al., 2003). It is known that Raldh1 has the lowest affinity for retinaldehyde and is less efficient in producing RA in cultured cells (Duester, 2000, Grün et al., 2000), and it has been suggested that this enzyme may be marginally involved in the RA synthetic pathway (Niederreither et al., 2002a). Comparing *Raldhs* and *Cyp26s* revealed several interesting trends with respect to temporal changes in expression. At E10, the expression level of *Cyp26A1* in the otocyst was strikingly high, about 20-fold higher than that of *Raldh3*, the *Raldh* with highest expression at this stage. *Cyp26B1* expression level was significantly lower than that of *Cyp26A1* (approximately 25% of the *Cyp26A1* level), yet it was much higher than the *Raldh2* or *-3* levels. These observations are confirmed by Western blot data where the two Raldh proteins investigated were barely detectable at E10, whereas Cyp26A1 protein was present (Fig. 3). The significantly higher level of *Cyp26s* compared to *Raldhs* at an early developmental stage suggests that restricting RA into very localized regions is essential for normal morphogenetic and organogenic events. However, *Cyp26A1* and *Cyp26B1* levels were sharply down-regulated after E14 and P5, respectively. In contrast, *Raldh 2* and*-3* expression was gradually up-regulated throughout development. At P20, the overall expression levels of *Raldh2* or *-3* in the inner ear were thus higher than those of *Cyp26A1* or *Cyp26B1*. Interestingly, the expression level of *Raldh3* in the cochlea was significantly higher than in the vestibular end organs, which was in striking contrast with the predominant expression of *Raldh2* in the vestibule vs. the cochlea. However, Western blot data would suggest a down regulation of Raldhs after birth The high level of transcripts and proteins of Raldhs suggests a role for RA signaling in later developmental events, such as differentiation and maturation of cells in the inner ear or may be involved in functional mechanisms of this sensory organ. The overall increase of RA levels later in development, along with the sharp down-regulation of the *Cyp26s*, also suggests that fully differentiated cells are more resistant to excess exposure to RA than undifferentiated or immature cells. The differential localization of Raldh2 and -3 to the vestibular and cochlear partitions of the inner ear, respectively, further suggests that expression of these enzymes is controlled by independent mechanisms.

Acknowledgments

We thank Drs Peter McCaffery and Ursula Dräger for providing Raldh2 and Raldh3 antibodies, Heather Aloor and Abdeljelil Jellali for technical assistance, and Prof. Pierre Chambon for his support.

Grant sponsor: This work was supported by funds from the Génopole de Strasbourg, the CNRS, the INSERM, the Collège de France, the Institut Universitaire de France, the Ministère de la Recherche, the Fondation pour la Recherche Médicale and the National Institutes of Health (DC005507).

NIH-PA Author Manuscript

NIH-PA Author Manuscript

NIH-PA Author Manuscript

Literature Cited

Abu-Abed S, Dollé P, Metzger D, Beckett B, Chambon P, Petkovich M. The retinoic acid-metabolizing enzyme, CYP26A1, is essential for normal hindbrain patterning, vertebral identity, and development of posterior structures. Genes Dev. 2001; 15:226–240. [PubMed: 11157778]

Achkar CC, Derguini F, Blumberg B, Langston A, Levin AA, Speck J, Evans RM, Bolado J Jr, Nakanishi K, Buck J, Gudas LJ. 4-Oxoretinol, a new natural ligand and transactivator of the retinoic acid receptors. Proc Natl Acad Sci U S A. 1996; 93:4879–4884. [PubMed: 8643497]

Berkovitz BK, Maden M, McCaffery P, Barrett AW. The distribution of retinaldehyde dehydrogenase-2 in rat and human orodental tissues. Arch Oral Biol. 2001; 46:1099–1104. [PubMed: 11684028]

Blentic A, Gale E, Maden. Retinoic acid signaling centers in the avian embryo identified by sites of expression of synthesizing and catabolising enzymes. Dev Dyn. 2003; 227:114–127. [PubMed: 12701104]

Burk DF, Willhite CC. Inner ear malformations induced by isotretinoin in hamster fetuses. Teratology. 1992; 46:147–157. [PubMed: 1440418]

Carson JP, Thaller Ch, Eichele G. A transcriptome atlas of the mouse brain at cellular resolution. Curr Opin Neurobiol. 2002; 12:562–565. [PubMed: 12367636]

Chambon P. A decade of molecular biology of retinoic acid receptors. FASEB J. 1996; 10:940–54. [PubMed: 8801176]

Chang BE, Blader P, Fischer N, Ingham PW, Strahle U. Axial HNF3beta and retinoic acid receptors are regulators of the zebrafish sonic hedgehog promoter. EMBO J. 1997; 16:3955–3964. [PubMed: 9233805]

Chang W, ten Dijke P, Wu DK. BMP pathways are involved in otic capsule formation and epithelial mesenchymal signaling in the developing chicken inner ear. Dev Biol. 2002; 251:380–394. [PubMed: 12435365]

Choo D, Sanne JL, Wu DK. The differential sensitivities of inner ear structures to retinoic acid during development. Dev Biol. 1998; 204:136–150. [PubMed: 9851848]

Colbert MC, Linney E, LaMantia AS. Local sources of retinoic acid coincide with retinoid-mediated transgene activity during embryonic development. Proc Nat Acad Sci USA. 1993; 90:6572–6576. [PubMed: 8341670]

Décimo, D.; Georges-Labouesse, E.; Dollé, P. *In situ* hybridization to cellular RNA. In: Hames, BD.; Higgins, SJ., editors. Gene probes 2, A practical approach. Oxford Univ Press; New York: 1995. p. 182-210.

Dudas M, Sridurongrit S, Nagy A, Okazaki K, Kaartinen V. Craniofacial defects in mice lacking BMP type I receptor Alk2 in neural crest cells. Mech Dev. 2002; 121:173–182. [PubMed: 15037318]

Duester G. Families of retinoid dehydrogenases regulating vitamin A function. Production of visual pigment and retinoic acid. Eur J Biochem. 2000; 267:4315–4324. [PubMed: 10880953]

Dupé V, Matt N, Garnier JM, Chambon P, Mark M, Ghyselinck NB. A newborn lethal defect due to inactivation of retinaldehyde dehydrogenase type 3 is prevented by maternal retinoic acid treatment. Proc Nat Acad Sci USA. 2003; 100:14036–14041. [PubMed: 14623956]

Fan X, Molotkov A, Manabe S, Donmoyer CM, Deltour L, Foglio MH, Cuenca AE, Blaner WS, Lipton SA, Duester G. Mol Cel Biol. 2003; 23:4637–4648.

Frenz DA, Galinovic-Schwartz V, Flanders FC, Van de Water TR. TGFβ_1 is an epithelial-derived signal peptide that influences otic capsule formation. Dev Biol. 1992; 153:324–336. [PubMed: 1397689]

Frenz DA, Liu W, Williams JD, Hatcher V, Galinovic-Schwartz V, Flanders KC, Van de Water TR. Induction of chondrogenesis: requirement for synergic interaction of basic fibroblast growth factor and transforming growth factor-beta. Development. 1994; 120:415–424. [PubMed: 8149917]

Frenz DA, Liu W, Galinovic-Schwartz V, Van de Water TR. Retinoic acid-induced embryopathy of the mouse inner ear. Teratology. 1996a; 53:292–303. [PubMed: 8879087]

Frenz DA, Liu W, Capparelli M. Role of BMP2 on otic capsule chondrogenesis. Ann NY Acad Sci. 1996b; 785:256–258. [PubMed: 8702146]

NIH-PA Author Manuscript

NIH-PA Author Manuscript

NIH-PA Author Manuscript

Frenz DA, Liu W. Effect of retinoic acid on otic capsule chondrogenesis in highdensity culture suggests disruption of epithelial-mesenchyme interactions. Teratology. 1997; 56:233–240. [PubMed: 9408973]

Frenz DA, Liu W. Treatment with all-*trans*-retinoic acid decreases levels of endogenous TGF-β_1 in the mesenchyme of the developing mouse inner ear. Teratology. 2000; 61:297–304. [PubMed: 10716749]

Fujii H, Sato T, Kaneko S, Gotoh O, Fijii-Kuriyama Y, Osawa K, Kato S, Hamada H. Metabolic inactivation of retinoic acid by a novel P450 differentially expressed in developing mouse embryos. EMBO J. 1997; 16:4163–4173. [PubMed: 9250660]

Jarvis BL, Johnston MC, Sulik KK. Congenital malformations of the external, middle and inner ear produced by isotretinoin exposure in mouse embryos. Otolaryng Head Neck Surg. 1990; 102:391–401.

Grün F, Hirose Y, Kawauchi S, Ogura T, Umesono T. Aldehyde dehydrogenase 6, a cytosolic retinaldehyde dehydrogenase prominently expressed in sensory neuroepithelia during development. J Biol Chem. 2000; 275:41210–41218. [PubMed: 11013254]

Gudas, LJ.; Sporn, MB.; Roberts, AB. Cellular biology and biochemistry of the retinoids. In: Sporn, MB.; Roberts, AB.; Goodman, DS., editors. The retinoids: biology, chemistry, and medicine. 2nd. Raven Press; New York: 1994. p. 443-520.

LaMantia AS. Forebrain induction, retinoic acid, and vulnerability to schizophrenia: insights from molecular and genetic analysis in developing mice. Biol Psychiatry. 1999; 46:19–30. [PubMed: 10394471]

Lanoue L, Dehart DB, Hinsdale ME, Maeda N, Tint GS, Sulik KK. Limb, genital, CNS, and facial malformations result from gene/environment-induced cholesterol deficiency: further evidence for a link to sonic hedgehog. Am J Med Genet. 1997; 73:24–31. [PubMed: 9375918]

Li H, Wagner E, McCaffery P, Smith D, Andreadis A, Dräger UC. A retinoic acid synthesizing enzyme in ventral retina and telencephalon of the embryonic mouse. Mech Dev. 2000; 95:283–289. [PubMed: 10906479]

Lin M, Zhang M, Abraham M, Smith SM, Napoli JL. Mouse retinal dehydrogenase 4 (RALDH4), molecular cloning, cellular expression, and activity in 9-cis-retinoic acid biosynthesis in intact cells. J Biol Chem. 2003; 278:9856–9861. [PubMed: 12519776]

Liu W, Oh SH, Kang YK, Li G, Doan TM, Little M, Li L, Ahn K, Crenshaw EB, Frenz DA. Bone morphogenetic protein 4 (BMP4): a regulator of capsule chondrogenesis in the developing mouse inner ear. Dev Dyn. 2003; 226:427–438. [PubMed: 12619129]

Luo T, Wagner E, Grün F, Dräger UC. Retinoic acid signaling in the brain marks formation of optic projections, maturation of the dorsal telencephalon, and function of limbic sites. J Comp Neurol. 2004; 470:297–316. [PubMed: 14755518]

Maden, M. Role of retinoids in embryonic development. In: Blomhoff, R., editor. Vitamin A in Health and Disease. Dekker; New York: 1994. p. 289-322.

Maden M. Retinoid signalling in the development of the central nervous system. Nature Rev Neurosci. 2002; 3:843–853. [PubMed: 12415292]

MacLean G, Abu-Abed S, Dollé P, Tahayato A, Chambon P, Petkovich M. Cloning of a novel retinoic acid-metabolizing cytochrome P450, Cyp26B1, and comparative expression analysis with Cyp26A1 during early murine development. Mech Dev. 2001; 107:195–201. [PubMed: 11520679]

McCaffery P, Wagner E, O'Neil J, Petkovitch M, Dräger UC. Dorsal and ventral retinal territories defined by retinoic acid synthesis, break-down and nuclear receptor expression. Mech Dev. 1999; 82:119–130. [PubMed: 10354476]

McCaffery P, Dräger UC. Regulation of retinoic acid signaling in the embryonic nervous system: A master differentiation factor. Cytokine Growth Factor Rev. 2000; 11:233–249. [PubMed: 10817966]

Mean AJ, Gudas LJ. The roles of retinoids in vertebrate development. Annu Rev Biochem. 1995; 64:201–233. [PubMed: 7574480]

Mic FA, Molotkox A, Fan X, Cuenca AE, Duester G. RALDH3, a retinaldehyde dehydrogenase that generates retinoic acid, is expressed in the ventral retina, otic vesicle and olfactory pit during mouse development. Mech Dev. 2000; 97:227–300. [PubMed: 11025231]

NIH-PA Author Manuscript

NIH-PA Author Manuscript

NIH-PA Author Manuscript

Mic FA, Duester G. Patterning of forelimb bud myogenic precursor cells requires retinoic acid signaling initiated by *Raldh2*. Dev Biol. 2003; 264:191–201. [PubMed: 14623241]

Morsli H, Choo D, Ryan A, Johnson R, Wu DK. Development of the mouse inner ear and origin of its sensory organs. J Neurosci. 1998; 18:3327–3335. [PubMed: 9547240]

Niederreither K, McCaffery P, Dräger UC, Chambon P, Dollé P. Restricted expression and retinoic acid-induced downregulation of the retinaldehyde type 2 (RALDH-2) gene during mouse development. Mech Dev. 1997; 62:67–78. [PubMed: 9106168]

Niederreither K, Dollé P. In situ hybridization with 35S-labeled probes for retinoid receptors. Methods Mol Biol. 1998; 89:247–267. [PubMed: 9664333]

Niederreither K, Subbarayan V, Dollé P, Chambon P. Embryonic retinoic acid synthesis is essential for early mouse post-implantation development. Nature Gen. 1999; 21:444–448.

Niederreither K, Vermot J, Fraulob V, Chambon P, Dollé P. Retinaldehyde dehydrogenase 2 (RALDH2)- independent patterns of retinoic acid synthesis in the mouse embryo. Proc Nat Acad Sci USA. 2002a; 99:16111–16116. [PubMed: 12454286]

Niederreither K, Abu-Abed S, Schuhbaur B, Petkovich M, Chambon P, Dollé P. Genetic evidence that oxidative derivatives of retinoic acid are not involved in retinoid signaling during mouse development. Nature Genet. 2002b; 31:84–88. [PubMed: 11953746]

Niederreither K, Fraulob V, Garnier JM, Chambon P, Dollé P. Differential expression of acid-synthesizing (RALDH) enzymes during fetal development and organ differentiation in the mouse. Mech Dev. 2002c; 110:165–171. [PubMed: 11744377]

Noden DM, Van de Water TR. Genetic analysis of mammalian ear development. Trends Neurosci. 1992; 15:235–237. [PubMed: 1381114]

Paradies NE, Sanford LP, Doetschman T, Friedman RA. Developmental expression of the TGFβs in the mouse cochlea. Mech Dev. 1998; 79:165–168. [PubMed: 10349630]

Pasqualetti M, Neun R, Davenne M, Rijli FM. Retinoic acid rescues inner ear defects in *Hoxa1* deficient mice. Nature Genet. 2001; 29:34–39. [PubMed: 11528388]

Perlmann T, Evans RM. Nuclear receptors in Sicily: all in the famiglia. Cell. 1997; 90:391–397. [PubMed: 9267019]

Perlmann, Th. Retinoid metabolism: a balancing act. Nat Gen. 2002; 31:7–8.

Pijnappel WW, Hendriks HF, Folkers GE, van den Brink CE, Dekker EJ, Edelenbosch C, van der Saag PT, Durston AJ. The retinoid ligand 4-oxo-retinoic acid is a highly active modulator of positional specification. Nature. 1993; 366:340–344. [PubMed: 8247127]

Riccomagno MM, Martinu L, Mulheisen M, Wu DK, Epstein DJ. Specification of the mammalian cochlea is dependant on sonic hedgehog. Genes Dev. 2002; 16:2365–2378. [PubMed: 12231626]

Romand R, Niederreither K, Abu-Abed S, Petkovich M, Fraulob V, Hashino E, Dollé P. Complementary expression patterns of retinoic acid-synthesizing and -metabolizing enzymes in prenatal mouse inner ear structures. Genes Exp Patt. 2004; 4:123–133.

Roos de K, Sonneveld E, Compaan B, Berge ten D, Durston AJ, Saag van der PT. Expression of retinoic acid 4-hydroxylase (CYP26) during mouse and *Xenopus laevis* embryogenesis. Mech Dev. 1999; 82:205–211. [PubMed: 10354487]

Ross SA, McCaffery PJ, Dräger UC, De Luca LM. Retinoids in embryonal development. Physiol Rev. 2000; 80:1021–1054. [PubMed: 10893430]

Rossant J, Zirngibl R, Cado D, Shago M, Giguere V. Expression of a retinoic acid response element-hsplacZ transgene defines specific domains of transcriptional activity during mouse embryogenesis. Genes Dev. 1991; 5:1333–1344. [PubMed: 1907940]

Sakai Y, Meno C, Fujji H, Nishino J, Shiratori H, Saijoh Y, Rossant J, Hamada H. The retinoic acid-inactivating enzyme CYP26 is essential for establishing an uneven distribution of retinoic acid along the anterio-posterior axis within the mouse embryo. Genes Dev. 2000; 15:213–225. [PubMed: 11157777]

Sakai Y, Meno C, Fujii H, Nishino J, Shiratori H, Saijoh Y, Rossant J, Hamada H. The retinoic acid-inactivating enzyme CYP26 is essential for establishing an uneven distribution of retinoic acid along the anterio-posterior axis within the mouse embryo. Genes Dev. 2001; 15:213–225. [PubMed: 11157777]

NIH-PA Author Manuscript

NIH-PA Author Manuscript

NIH-PA Author Manuscript

Sakai Y, Luo T, McCaffery P, Hamada H, Dräger UC. CYP26A1 and CYP26C1 cooperate in degrading retinoic acid within the equatorial retina during later eye development. Dev Biol. 2004; 276:143–157. [PubMed: 15531370]

Sizemore N, Choo CK, Eckert RL, Rorke EA. Transcriptional regulation of the EGF receptor promoter by HPV16 and retinoic acid in human ectocervical epithelial cells. Exp Cell Res. 1998; 244:349–356. [PubMed: 9770378]

Stoilov I. Cytochrome P450s: coupling development and environment. Trends Genet. 2001; 17:629–632. [PubMed: 11672862]

te Welscher P, Zuniga A, Kuipers S, Drenth T, Goedemans HJ, Meijlink F, Zeller R. Progression of vertebrate limb development through SHH-mediated counteraction of GLI3. Science. 2002; 29:827–830. [PubMed: 12215652]

Thompson DL, Gerlach-Bank LM, Barald KF, Koening RJ. Retinoic acid repression of bone morphogenetic protein 4 in inner ear development. Mol Cell Biol. 2003; 23:2277–2286. [PubMed: 12640113]

Underhill TM, Sampalo AV, Weston AD. Retinoid signalling and skeletal development. Novartis Found Symp. 2001; 232:171–185. [PubMed: 11277079]

Yoshizawa M, Miyazaki H, Kojima S. Retinoids potentiate transforming growth factor-beta activity in bovine endothelial cells through up-regulating the expression of transforming growth factor-beta receptors. J Cell Physiol. 1998; 176:565–573. [PubMed: 9699509]

Vermot J, Niederreither K, Garnier JM, Chambon P, Dollé P. Decreased embryonic retinoic acid synthesis results in a DiGeorge syndrome phenotype in newborn mice. Proc Nat Acad Sci USA. 2003; 100:1763–1768. [PubMed: 12563036]

Wagner E, Luo T, Dräger UC. Retinoic acid synthesis in the postnatal mouse brain marks distinct developmental stages and functional systems. Cerebral Cortex. 2002; 12:1244–1253. [PubMed: 12427676]

White JA, Beckett-Jones B, Guo YD, Dilworth FJ, Bonasoro J, Jones G, Petkovich M. cDNA cloning of human retinoic acid-metabolizing enzyme (hP450RAI) identifies a novel family of cytochromes P450 (CYP26). J Biol Chem. 1997; 272:18538–18541. [PubMed: 9228017]

White JA, Ramshaw H, Taimu M, Stangle W, Zhang A, Everingham S, Creigton S, Tam SP, Jones G, Petkovich M. Identification of the human cytochrome P450, P450RAI-2, which is predominantly expressed in the adult cerebellum and is responsible for all-*trans*-retinoid acid metabolism. Proc Nat Acad Sci USA. 2000; 97:6403–6408. [PubMed: 10823918]

Wright, TJ.; Mansour, SL. FGF signaling in ear development and innervation In: Development of Auditory and Vestibular Systems-3. In: Romand, R.; Varela-Nieto, I., editors. Current Topics in Developmental Biology. Vol. 57. Elsevier Acad Press; San Diego: 2003. p. 225-259.

Yashiro K, Zhao X, Uehara M, Yamashita K, Nishijima M, Nishino J, Saijoh Y, Sakai Y, Hamada H. Regulation of retinoic acid distribution is required for proximodistal patterning and outgrowth of the developing mouse limb. Dev Cell. 2004; 6:411–422. [PubMed: 15030763]

NIH-PA Author Manuscript

NIH-PA Author Manuscript

NIH-PA Author Manuscript

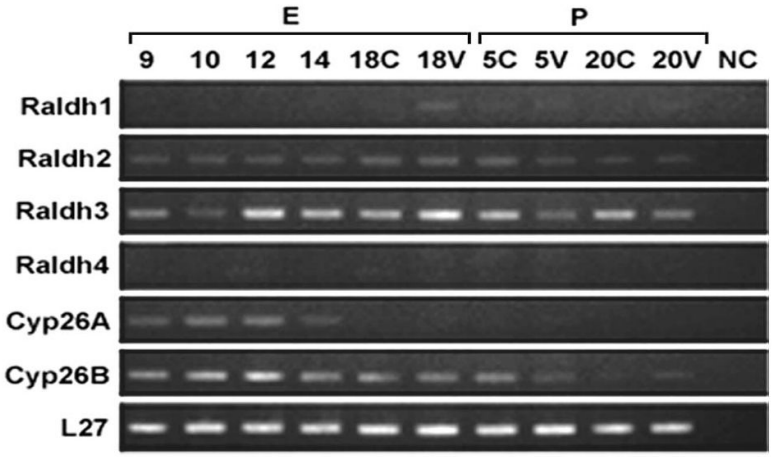

Figure 1.

RT-PCR analysis of mRNAs of RA synthesizing enzymes (*Raldh1-4*) and –metabolizing enzymes (*Cyp26A1* and *Cyp26B1*) in dissected inner ear samples. All enzymes, except *Raldh4*, were expressed at some stage in the developing inner ear, but their expression levels varied according to the stage analyzed. Of all *Raldhs*, *Raldh4* was undetectable already at the earliest stage investigated (E9), while *Raldh3* mRNA level was highest, followed by *Raldh2*. *Raldh1* mRNA expression was very low at early stages, but was up-regulated at E18. A graded up-regulation of *Raldh2* from E9 to E18 was observed, followed by a down-regulation after birth, while *Raldh3* was steadily expressed from E9 to P20, albeit at lower levels in the vestibular component after birth. *Cyp26A1* mRNA was detectable up to E14, while down-regulation started at P5 for *Cyp26B1* in the vestibular region of the inner ear and later for the cochlear component. *L27* mRNA, which encodes for a housekeeping gene, is analyzed as an internal control. C: cochlear tissues; V: vestibular tissues; E: embryonic stage; P: postnatal stage; NC: negative control.

NIH-PA Author Manuscript
NIH-PA Author Manuscript
NIH-PA Author Manuscript

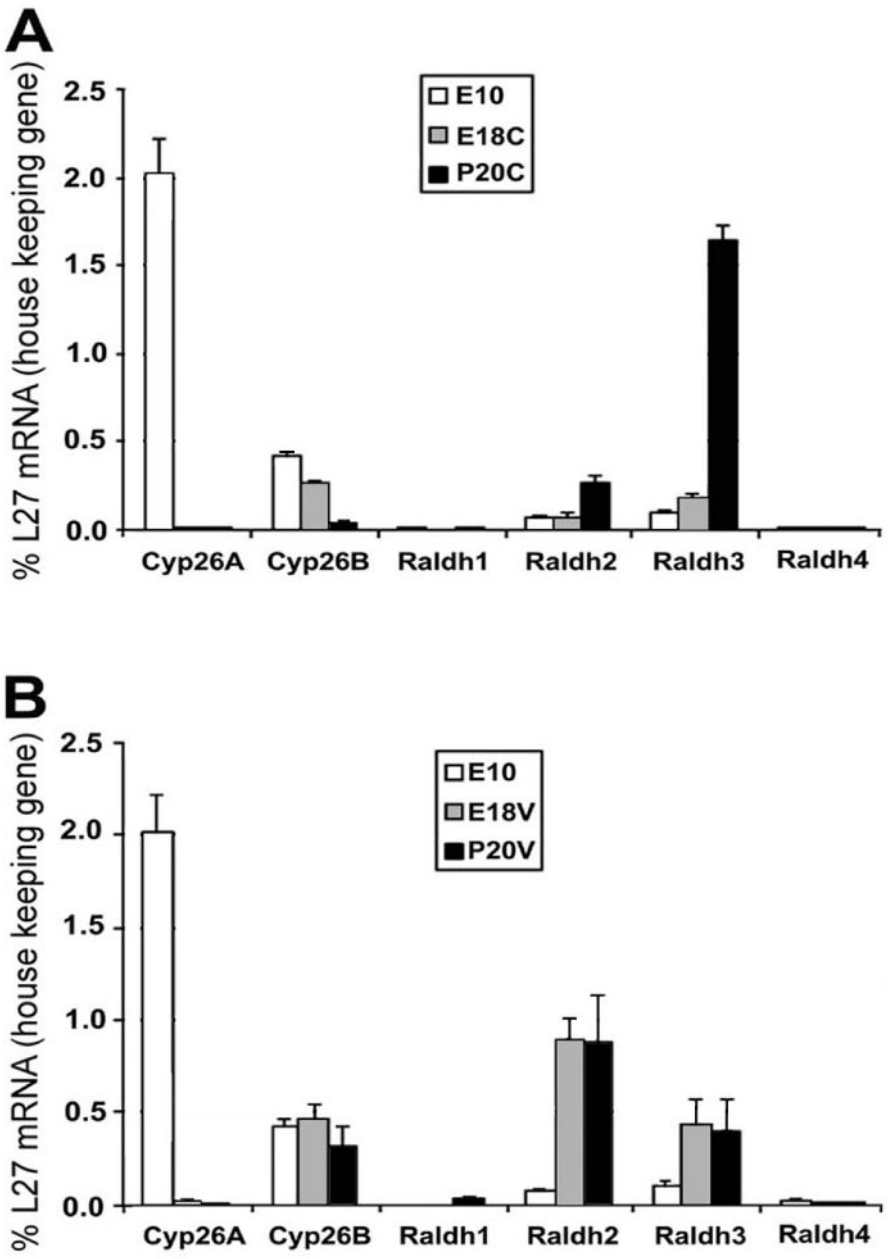

Figure 2.

Quantitative RT-PCR analysis for *Raldh1-4* and *Cyp26A1* and --*B1* at two prenatal stages (E10 and E18.5) and one postnatal stage (P20) in cochlear (A) and vestibular tissues (B). At E10 it was not possible to separate cochlear from vestibular tissues. From this quantitative observation, one can see that *Cyp26* transcripts are strongly expressed at E10 but are down regulated thereafter. *Raldh* transcripts, especially *Raldh2* and *–3* are well expressed in postnatal inner ear, with a stronger expression for *Raldh3* in the cochlear tissues and *Raldh2* in the vestibular ones. Each vertical bar represents an mRNA level (+/- S.D.) relative to the L27 level (internal control).

NIH-PA Author Manuscript

NIH-PA Author Manuscript

NIH-PA Author Manuscript

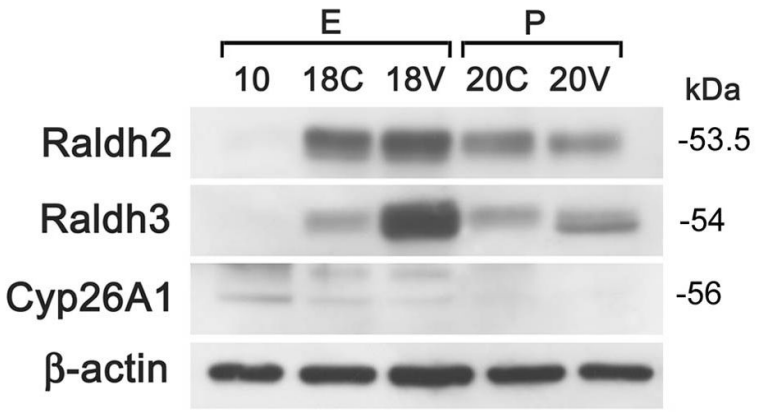

Figure 3.

Western blot analysis of Raldh2, Raldh3 and Cyp26A1 in inner ear tissues at E10, E18 or P20. Raldh2 and Raldh3 are barely detectable at E10, after which they are up-regulated at E18 in both cochlear (C) and vestibular (V) partitions. Raldh3 is more strongly expressed in the vestibular partition compared to the cochlear partition. Cyp26A1 is clearly expressed at E10, but is down-regulated at E18 for both partitions and is hardly detectable by P20. A β-actin antibody was used as internal control. Whether the weak intensity of the Cyp26A1 bands in comparison to the Raldhs reflects a relatively weak affinity of the antibody, rather than actual lower protein levels, cannot be ascertained.

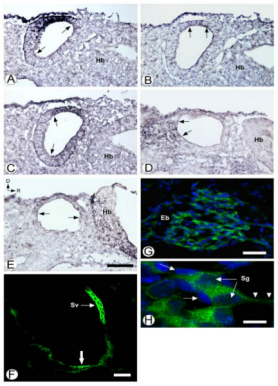

Figure 4.

ISH of *Raldhs* and *Cyp26s* on sagittal sections of E9.5 otocysts (A-E) and immunohistochemistry of Raldh2 and -3 in the E18.5 cochlea (F-H). *Raldh* transcripts, when present, are restricted to the otic epithelium. *Raldh1* is localized in the dorsal otocyst extending toward the caudal direction (A), whereas *Raldh2* is localized in a restricted region of the dorsal otocyst (B). *Raldh3* extends ventrally towards the rostral region as depicted by arrows (C), which demarcate the territory of enzymes expression.. *Cyp26A1* is present in caudal and ventral mesenchyme and restricted to a small caudal region of the otic epithelium (arrows) (D). *Cyp26B1* is present in the upper half of the otic epithelium (E).

Raldh2 protein immunohistochemistry shows expression in the stria vascularis (Sv) and likely in the apical region of hair cells (large arrow) (F). G-H: Raldh3 protein expression in the spiral ganglion cell bodies (green) is restricted to the cytoplasm of the ganglion cells extending to its central process (arrowheads). No expression is present in the nearby satellite cell nuclei (blue, DAPI labeling) (arrows) and fibers of the efferent bundle (Eb). D: dorsal, Hb: hindbrain, R: rostral. Scale bar: 10 μm (A-E), 50 μm (F), 100 μm (G), 20 μm (H).

NIH-PA Author Manuscript NIH-PA Author Manuscript NIH-PA Author Manuscript

NIH-PA Author Manuscript

NIH-PA Author Manuscript

NIH-PA Author Manuscript

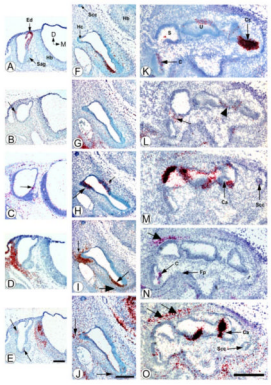

Figure 5.

A-E: Expression of *Raldh1, -2, 3* and *Cyp26A1* and *-B1* in the E10.5 otocyst. *Raldh1* transcripts are localized to the endolymphatic duct primordium and the upper medial region of the otocyst (A), while *Raldh2* (B) exhibits restricted expression in the lateral region of the otocyst (arrow). *Raldh3* transcripts (C) are limited to a small area in the medial region (arrow). *Cyp26A1* is strongly expressed in the adjacent mesenchyme and more weakly in the ventro-lateral otocyst epithelium (D). *Cyp26B1* transcripts (E) are restricted to two small regions in the lateral and ventro-medial parts of the otocyst epithelium (arrows). Expression is weaker than in the adjacent hindbrain neuroepithelium. No ISH signal is visible in the stato-acoustic ganglion, whatever the enzymes.

F-J: Expression of *Raldh1, 2* and *-3*, and *Cyp26A1* and *-B1* in the differentiating otocyst at E12.5. *Raldh1* expression is seen in the ventral region of the inner ear at the opposite side of the prospective sensory epithelium of the cochlea (F). *Raldh2* mRNA is not observed on this section (G). *Raldh3* transcripts (H) are present in the prospective vestibular sensory epithelium (small arrow) and the epithelium close to the horizontal semi-circular canal (large arrow). *Cyp26A1* transcripts (I) are detected in the prospective cochlea opposite to the sensory epithelium (arrow), and in mesenchyme around the horizontal canal (small arrow). Weak signal is detected in the mesenchyme surrounding the cochlea (large arrow). Weak *Cyp26B1* ISH signals are restricted to mesenchymal tissues around the horizontal semi-circular canal and the cochlea (arrows) (J).

K-O: Expression of *Raldh1, -2* and *-3*, and *Cyp26A1* and *-B1* in the E14.5 inner ear. In this section, *Raldh1* transcripts (K) are localized in the cochlear canal, the utricule and are strongly expressed in the crus commune, while *Raldh2* (L) exhibits restricted expression in the mesenchyme between the saccule and the cochlea (arrow). Weak expression is also visible close to the utricule and a semi-circular canal (arrowhead). *Raldh3* transcripts are observed in the saccule, the utricule and cells close to the cristae ampullaris (M). *Cyp26A1* expression (N) is present in the cochlea and below the sensory epithelium of the saccule, presumably in vestibular ganglion cells (large arrow). *Cyp26B1* transcripts (O) are localized to the utricule and the cristae ampullaris, and below the saccule and utricule (large arrows).

C: cochlea, Ca: cristae ampullaris, Cc: crus commune, D: dorsal, Ed: endolymphatic duct, Fp: foot plate of the stapes, Hb: hindbrain, Hc: horizontal semi-circular canal, S: saccule, Sag: stato-acoustic and facial ganglion complex, Scc: semi-circular canal, U: utricule, M: medial. Scale bar: 200 μm (A-J), 300 μm (K-O).

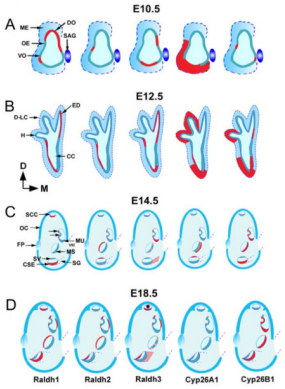

Figure 6.

Schematics of *Raldhs* and *Cyp26s* expression patterns in the E10.5 (A), E12.5 (B), E14.5 (C) and E18.5 (D) inner ear. Briefly at E10.5 and E12.5 (see Results for full descriptions), *Raldhs* are only present in vestibular and/or cochlear epithelium, while *Cyp26* transcripts are mainly expressed in mesenchymal areas. Only *Cyp26A1* is observed at E10.5, while both *Cyp26* enzymes are present two days later. At E12.5 both *Cyp 26* transcripts partly overlap in the cochlear canal and the horizontal semi-circular canal.

At E14.5 (C) and E18.5 (D), *Raldh1* transcripts are present in all three semi-circular canals, in the transitional epithelium of the utricular macula and cristae and in different cochlear epithelia except sensory hair cells. *Raldh2* is mainly expressed in the dark cell region of the vestibular component of the inner ear, the stria vascularis and the Reissner membrane of the cochlea. *Raldh3* is observed in a single semi-circular canal (asterisk), the transitional epithelium of cristae, the lateral regions of the saccule and utricule extending toward the sensory epithelium, the spiral ganglion and the stria vascularis. *Cyp26A1* transcripts are restricted to two regions of the E14.5 inner ear, but are no longer detected two days later, while *Cyp26B1* transcripts are seen in the sensory epithelia of the utricule, the saccule, cristae and the cochlea, but not in sensory cells.

CA: crista ampullaris, CC: cochlear canal, CSE: cochlear sensory epithelium, D. dorsal, D-LC: dorsal and lateram semi-circular canal, DO: dorsal otocyst including the endolymphatic duct, ED: endolymphatic duct, FP: foot plate of the staples, H: horizontal semi-circular canal, LCA: lateral epithelium of the crista ampullaris, M: medial, ME: mesenchyme, MU: macule of the utricule, MS: macule of the saccule, OC: otic capsule, OE: otic epithelium, SCC: semicircular canals, SCE: cochlear sensory epithelium, SG: spiral ganglion, SV: stria vascularis, VO: ventral otocyst inclusing the cochlear canal. VIII: stato-acoustic nerve.

NIH-PA Author Manuscript NIH-PA Author Manuscript NIH-PA Author Manuscript